

Zn(II) Coordination to Polyamine Macrocycles Containing Dipyridine Units. New Insights into the Activity of Dinuclear Zn(II) Complexes in Phosphate Ester Hydrolysis

Carla Bazzicalupi, Andrea Bencini,* Emanuela Berni, Antonio Bianchi,* Patrizia Fornasari, Claudia Giorgi, and Barbara Valtancoli

Department of Chemistry, University of Florence, Via della Lastruccia 3, Sesto Fiorentino, Firenze, Italy

Received February 25, 2004

Zn(II) binding by the dipyridine-containing macrocycles L1-L3 has been analyzed by means of potentiometric measurements in aqueous solutions. These ligands contain one (L1, L2) or two (L3) 2,2'-dipyridine units as an integral part of a polyamine macrocyclic framework having different dimensions and numbers of nitrogen donors. Depending on the number of donors, L1-L3 can form stable mono- and/or dinuclear Zn(II) complexes in a wide pH range. Facile deprotonation of Zn(II)-coordinated water molecules gives mono- and dihydroxo-complexes from neutral to alkaline pH values. The ability of these complexes as nucleophilic agents in hydrolytic processes has been tested by using bis(*p*-nitrophenyl) phosphate (BNPP) as a substrate. In the dinuclear complexes the two metals play a cooperative role in BNPP cleavage. In the case of the L2 dinuclear complex $[Zn_2L2(OH)_2]^{2+}$, the two metals act cooperatively through a hydrolytic process involving a bridging interaction of the substrate with the two Zn(II) ions and a simultaneous nucleophilic attack of a Zn-OH function at phosphorus; in the case of the dizinc complex with the largest macrocycle L3, only the monohydroxo complex $[Zn_2L3(OH)]^{3+}$ promotes BNPP hydrolysis. BNPP interacts with a single metal, while the hydroxide anion may operate a nucleophilic attack. Both complexes display high rate enhancements in BNPP cleavage with respect to previously reported dizinc complexes, due to hydrophobic and π -stacking interactions between the nitrophenyl groups of BNPP and the dipyridine units of the complexes.

Introduction

Over the years a great deal of interest has been focused on the role of metal ions in the active centers of hydrolytic metalloenzymes.^{1–10} Many hydrolytic enzymes, including those which hydrolyze the phosphate ester bond, contain a

couple of Zn(II) ions in their active site, which act cooperatively in the catalytic process. The role of zinc is generally due to binding and activation of the substrates; at the same time, deprotonation of Zn(II)-coordinated water molecules give Zn-OH functions, which act as nucleophilic agents in the hydrolytic mechanism. The catalytic site can be lodged in a hydrophobic pocket, which may contribute to substrate binding and can also assist the formation of the nucleophilic Zn(II)-OH functions.

Polyamine macrocycles containing six or more nitrogen donors and cavities of appropriate shape and dimension may be able to hold two metal centers at short distances.^{11–24} The

* Author to whom correspondence should be addressed. Tel: 0039-055-4573371. Fax: 0039-055-4573364. E-mail: andrea.bencini@unifi.it.

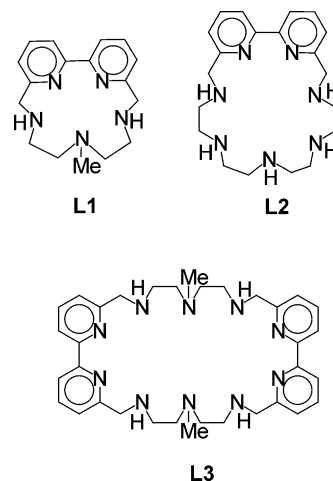
- (1) *Zinc Enzymes*; Bertini, I., Luchinat, C., Marek, W., Zeppezauer, M., Eds.; Birkhauser: Boston, MA, 1986.
- (2) Kim, E. E.; Wyckoff, H. W. *J. Mol. Biol.* **1991**, *218*, 449–464.
- (3) Coleman, J. E. *Annu. Rev. Biophys. Biomol. Struct.* **1992**, *21*, 441–483.
- (4) (a) Lipscomb, W. N.; Sträter, N. *Chem. Rev.* **1996**, *96*, 2375–2434. (b) Sträter, N.; Lipscomb, W. N.; Klabunde, T.; Krebs, B. *Angew. Chem., Int. Ed. Engl.* **1996**, *35*, 2024–2055.
- (5) Wilcox, D. E. *Chem. Rev.* **1996**, *96*, 2435–2458.
- (6) Steinhagen, H.; Helmchem, G. *Angew. Chem., Int. Ed. Engl.* **1996**, *35*, 2339–2342.
- (7) Dodgson, S. J.; Tashian, R. E.; Gros, G.; Carter, N. D. *The Carbonic Anhydrases*; Plenum Press: New York, 1991.
- (8) Christianson, D. W. *Adv. Protein Chem.* **1991**, *41*, 281–355.
- (9) Silverman, D. N.; Lindskog, S. *Acc. Chem. Res.* **1988**, *21*, 30–36.
- (10) Holz, R. C. *Coord. Chem. Rev.* **2002**, *232*, 5–26.

- (11) (a) *Chemistry of Heterocyclic Compounds, Vol. 51: Aza-Crown Macrocycles*; Bradshaw, J. S., Krakowiak, K. E., Izatt, R. M., Eds.; Wiley: New York, 1993. (b) Izatt, R. M.; Pawlak, K.; Bradshaw, J. S.; Bruening, R. L. *Chem. Rev.* **1995**, *95*, 2529–2586.
- (12) Lehn, J.-M. *Supramolecular Chemistry: Concepts and Perspectives*; VCH: New York, 1995.
- (13) (a) Lindoy, L. F. *The Chemistry of Macrocyclic Ligand Complexes*; Cambridge University Press: Cambridge, UK, 1992. (b) Lindoy, L. F. *Pure Appl. Chem.* **1997**, *69*, 2179–2184.

distance between the two metal ions can be varied by an opportune synthetic modulation of the dimension of the macrocyclic cavity and of the ligand flexibility. At the same time, the chemical properties of the metal centers depend on the ligational properties of the chelating sites, and, therefore, an appropriate design of the metal binding unit may lead to polynuclear metal complexes with different reactivity and catalytic properties. For these reasons, several dinuclear Zn(II) complexes with polyazamacrocycles have been used to mimic the multinuclear metal arrays at the active sites of hydrolytic metallo-enzymes.^{25–42}

We have recently described the synthesis of a new series of dipyrindine-containing polyaza macrocycles, such as L1–L3.⁴³

The dipyrindine unit of these ligands possesses two nitrogen donors whose unshared electron pairs are beautifully placed



- (14) (a) Raidt, R.; Neuburger, M.; Kaden, T. A. *Dalton Trans.* **2003**, 1292–1298. (b) Kaden, T. A. *Coord. Chem. Rev.* **1999**, 190–192, 371–389.
- (15) Nelson, J.; McKee, V.; Morgan, G. *Progr. Inorg. Chem.* **1998**, 47, 167–316.
- (16) Bencini, A.; Bianchi, A.; Paoletti, P.; Paoli, P. *Coord. Chem. Rev.* **1992**, 120, 51–85.
- (17) (a) Fry, F. H.; Fallon, G. D.; Spiccia, L. *Inorg. Chim. Acta* **2003**, 346, 57–66. (b) Fry, F. H.; Jensen, P.; Kepert, C. M.; Spiccia, L. *Inorg. Chem.* **2003**, 42, 5637–5644. (c) Fry, F. H.; Moubarak, B.; Murray, K. S.; Spiccia, L.; Warren, M.; Skelton, B. W.; White, A. H. *J. Chem. Soc., Dalton Trans.* **2003**, 866–871. (d) Brudenell, J. S.; Spiccia, L.; Hockless, D. C. R.; Tiekink, E. R. T. *J. Chem. Soc., Dalton Trans.* **1999**, 1475–1482.
- (18) (a) Depree, C. V.; Beckmann, U.; Heslop, K.; Brooker, S. D. *J. Chem. Soc., Dalton Trans.* **2003**, 3469–3476. (b) Brooker, S. D. *Coord. Chem. Rev.* **2001**, 222, 3–30.
- (19) (a) Lamarque, L.; Miranda, C.; Navarro, P.; Escartí, F.; García-España, E.; LaTorre, J.; Ramírez, J. A. *Chem. Commun.* **2000**, 1337–1338. (b) Lamarque, L.; Navarro, P.; Miranda, C.; Aran, V. J.; Ochoa, C.; Escartí, F.; García-España, E.; LaTorre, J.; Luis, S. V.; Miravet, J. F. *J. Am. Chem. Soc.* **2001**, 123, 10560–10570.
- (20) Guerriero, P.; Tamburini, S.; Vigato, P. A. *Coord. Chem. Rev.* **1995**, 139, 17–243.
- (21) (a) Hortala, M. A.; Fabbrizzi, L.; Marcotte, N.; Stomeo, F.; Taglietti, A. *J. Am. Chem. Soc.* **2003**, 125, 20–21. (b) Amendola, V.; Bastianello, E.; Fabbrizzi, L.; Mangano, C.; Pallavicini, P.; Perotti, A.; Manotti-Lanfredi, A.; Ugozzoli, F. *Angew. Chem., Int. Ed.* **2000**, 39, 2917–2920.
- (22) (a) Ambrosi, G.; Dapporto, P.; Formica, M.; Fusi, V.; Giorgi, L.; Guerri, A.; Micheloni, M.; Paoli, P.; Pontellini, R.; Rossi, P. *Chem. Eur. J.* **2003**, 9, 800–810. (b) Dapporto, P.; Formica, M.; Fusi, V.; Giorgi, L.; Micheloni, M.; Paoli, P.; Pontellini, R.; Rossi, P. *Inorg. Chem.* **2001**, 40, 6186–6192.
- (23) Chand, D. K.; Schneider, H.-J.; Bencini, A.; Bianchi, A.; Giorgi, C.; Ciattini, S.; Valtancoli, B. *Chem. Eur. J.* **2000**, 6, 4001–4007.
- (24) (a) Adams, H.; Clunas, S.; Fenton, D. E.; Spey, S. E. *Dalton Trans.* **2003**, 625–630. (b) Ōkawa, H.; Furutachi, H.; Fenton, D. E. *Coord. Chem. Rev.* **1998**, 174, 51–75.
- (25) Schneider H.-J.; Yatsimirsky, A. In *Metal Ion in Biological Systems*; Sigel, H., Sigel, A., Eds.; Marcel Dekker: New York, 2003; Vol. 40, pp 369–462.
- (26) Blasko, A.; Bruice, T. C. *Acc. Chem. Res.* **1999**, 32, 475–484 and references therein.
- (27) Hegg, E. L.; Burstyn, J. N. *Coord. Chem. Rev.* **1998**, 173, 133–165 and references therein.
- (28) Krämer, R. *Coord. Chem. Rev.* **1999**, 182, 243–261 and references therein.
- (29) (a) Kimura, E. *Curr. Op. Chem. Biol.* **2000**, 4, 207–213. (b) Aoki, S.; Kimura, E. *Rev. Mol. Biotech.* **2002**, 90, 129–155 and references therein. (c) Kimura, E.; Koike, T. *Inorg. Chem.* **1997**, 44, 2229–261. (d) Kimura, E.; Koike, T. *J. Chem. Soc., Chem. Commun.* **1998**, 1495–1500.
- (30) Fenton D. E.; Ōkawa H. *Chem. Ber.* **1997**, 130, 433–442.
- (31) (a) Molenveld, P.; Engbersen, J. F. J.; Reinhoudt, D. N. *Chem. Soc. Rev.* **2000**, 29, 75–86. (b) Molenveld, P.; Stikvoort, W. M. G.; Kooijman, H.; Spek, A. L.; Engbersen, J. F. J.; Reinhoudt, D. N. *J. Org. Chem.* **1999**, 64, 3896.

to bind metal cations. At the same time, the rigidity of the dipyrindine moiety would give an overall stiffening of the macrocyclic structures, leading to a high degree of preorganization in metal coordination. Finally, this heteroaromatic unit is also rather hydrophobic and would generate a hydrophobic environment for the coordinated metals. All these factors can influence the binding properties of the ligands for Zn(II) as well as the reactivity of the generated complexes in hydrolytic reactions. These considerations prompted us to carry out a solution and X-ray structural investigation on Zn(II) binding with L1–L3. The hydrolytic

- (32) (a) Rossi, P.; Felluga, F.; Tecilla, P.; Formaggio, F.; Crisma, M.; Toniolo, C.; Scrimin, P. *Biopolymers* **2000**, 55, 496–501. (b) Sissi, C.; Rossi, P.; Felluga, F.; Formaggio, F.; Palumbo, M.; Tecilla, P.; Toniolo, C.; Scrimin, P. *J. Am. Chem. Soc.* **2001**, 123, 3169–3170.
- (33) (a) Iranzo, O.; Kovalevsky, A. Y.; Morrow, J. R.; Richard, J. P. *J. Am. Chem. Soc.* **2003**, 125, 1988–1993. (b) Iranzo, O.; Elmer, T.; Richard, J. P.; Morrow, J. R. *Inorg. Chim. Acta* **2003**, 42, 7737–7746. (c) Yang, M.-Y.; Richard, J. P.; Morrow, J. R. *Chem. Commun.* **2003**, 2832–2833.
- (34) (a) Jurek, P.; Martell, A. E. *Inorg. Chim. Acta* **1999**, 287, 47–51. (b) Luiz, M. T. B.; Szpoganicz, B.; Rizzoto, M.; Basallote, M. G.; Martell, A. E. *Inorg. Chim. Acta* **1999**, 287, 134–141. (c) Kong, D.; Martell, A. E.; Reibenspies, J. *Inorg. Chim. Acta* **2002**, 333, 7–14.
- (35) (a) Chapman, W. H., Jr.; Breslow, R. *J. Am. Chem. Soc.* **1995**, 117, 5462–5469. (b) Leivers, M.; Breslow, R. *Bioorg. Chem.* **2001**, 29, 345–356.
- (36) Schneider H.-J.; Hettich, R. *J. Am. Chem. Soc.* **1997**, 119, 5638–5647.
- (37) (a) Bazzicalupi, C.; Bencini, A.; Bianchi, A.; Fusi, V.; Giorgi, G.; Paoletti, P.; Valtancoli, B.; Zanchi, D. *Inorg. Chem.* **1997**, 36, 2784–2790. (b) Bazzicalupi, C.; Bencini, A.; Berni, E.; Bianchi, A.; Fedi, V.; Fusi, V.; Giorgi, G.; Paoletti, P.; Valtancoli, B. *Inorg. Chem.* **1999**, 38, 4115–4122. (c) Bazzicalupi, C.; Bencini, A.; Berni, E.; Bianchi, A.; Giorgi, G.; Paoletti, P.; Valtancoli, B. *Inorg. Chem.* **1999**, 38, 6323–6325.
- (38) Nihan, F.; Akkaya, M. S.; Akkaya, E. U. *J. Mol. Catal. A: Chem.* **2001**, 165, 291–294.
- (39) (a) Li, S.-A.; Yang, D.-X.; Li, D.-F.; Huang, J.; Tang, W.-X. *New J. Chem.* **2002**, 26, 1831–1837. (b) Li, S.-A.; Li, D. F.; Yang, D.-X.; Li, Y.-Z.; Huang, J.; Yu, K.-B.; Tang, W.-X. *Chem. Commun.* **2003**, 7, 880–881. (c) Yang, D.-X.; Li, S.-A.; Li, D.-F.; Xia, J.; Yu, K.-B.; Tang, W.-X. *J. Chem. Soc., Dalton Trans.* **2002**, 4042–4047.
- (40) Vichard, C.; Kaden, T. A. *Inorg. Chim. Acta* **2002**, 337, 173–180.
- (41) (a) Kimura, E.; Kikuchi, M.; Kitamura, H.; Koike, T. *Chem. Eur. J.* **1999**, 5, 3113–3123. (b) Koike, T.; Takashige, M.; Kimura, E.; Fujioka, H.; Shiro, M. *Chem. Eur. J.* **1996**, 2, 617–623. (c) Aoki, S.; Sugimura, C.; Kimura, E. *J. Am. Chem. Soc.* **1998**, 120, 10094–10102. (d) Koike, T.; Inoue, M.; Kimura, E.; Shiro, M. *J. Am. Chem. Soc.* **1996**, 118, 3091–3099.
- (42) (a) Gajda, T.; Kramer, R.; Jancso, A. *Eur. J. Inorg. Chem.* **2000**, 1635–1644. (b) Jancso, A.; Mikkola, S.; Lönnberg, H.; Hegetschweiler, K.; Gajda, T. *Chem. Eur. J.* **2003**, 9, 5404–5415.

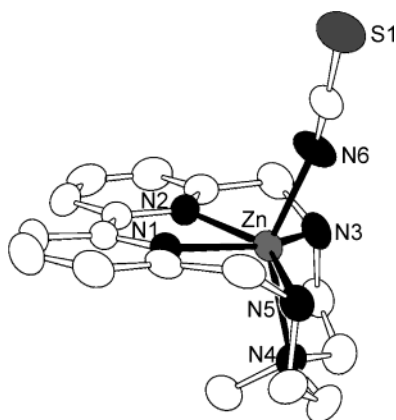


Figure 1. ORTEP drawing of the $[\text{ZnL1}(\text{NCS})]^+$ cation (1).

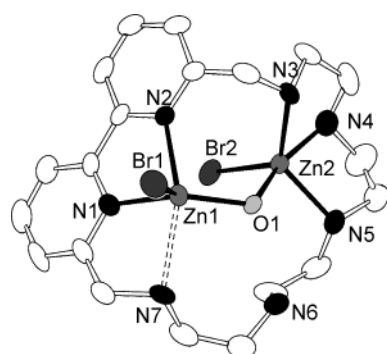


Figure 2. ORTEP drawing of the $[\text{Zn}_2(\text{L2H})(\mu\text{-OH})\text{Br}_2]^{2+}$ cation (3).

ability of the complexes was then tested by using bis(*p*-nitrophenyl) phosphate (BNPP) as substrate.

Results and Discussion

Synthesis and Crystal Structures of $[\text{ZnL1}(\text{NCS})]\text{ClO}_4$ (1), $[\text{Zn}_2(\text{L2H})(\mu\text{-OH})\text{Br}_2](\text{ClO}_4)\text{Br}$ (3), and $[\text{Zn}_2\text{L3I}_2](\text{ClO}_4)_2 \cdot 2\text{H}_2\text{O}$ (6). Crystals suitable for single-crystal X-ray analysis were obtained by slow evaporation of an aqueous solution containing Zn(II) and L1 in a 1:1 molar ratio and an excess of SCN^- ($[\text{ZnL1}(\text{NCS})]\text{ClO}_4$ (1) or from water solutions containing the preformed dinuclear Zn(II) complexes $[\text{Zn}_2\text{L2}](\text{ClO}_4)_4 \cdot 4\text{H}_2\text{O}$ (2) or $[\text{Zn}_2\text{L3}](\text{ClO}_4)_4 \cdot 2\text{H}_2\text{O}$ (5) in the presence of NaBr ($[\text{Zn}_2(\text{L2H})(\mu\text{-OH})\text{Br}_2](\text{ClO}_4)\text{Br}$, 3) or NaI ($[\text{Zn}_2\text{L3I}_2](\text{ClO}_4)_2 \cdot 2\text{H}_2\text{O}$, 6).

The X-ray crystal structure of the mononuclear complex 1 shows the metal hexacoordinated by the five nitrogens of the ligand and an NCS^- anion within a strongly distorted octahedral environment (Figure 1 and Table 1). The equatorial plane of the coordination octahedron is defined by the heteroaromatic nitrogens N1 and N2 and the benzylic amine groups N3 and N5 (max deviation 0.015(5) Å for N2), while the apical positions are occupied by the methylated amine group N4 and the N6 nitrogen of the isothiocyanate anion (N6–Zn–N4 143.48(2)°). The metal is 0.1359(7) Å displaced out of the basal plane in the direction of the N6 donor.

Table 1. Selected Bond Angles (deg) and Distances (Å) for Metal Coordination Environment in $[\text{ZnL1}(\text{NCS})]\text{ClO}_4$ (1)

Zn–N1	2.182(5)	Zn–N4	2.200(5)
Zn–N2	2.152(5)	Zn–N5	2.332(5)
Zn–N3	2.270(5)	Zn–N6	2.033(5)
N1–Zn–N2	73.0(2)	N2–Zn–N6	103.9(2)
N1–Zn–N3	147.1(2)	N3–Zn–N4	79.2(2)
N1–Zn–N4	106.6(2)	N3–Zn–N5	139.4(2)
N1–Zn–N5	72.3(2)	N3–Zn–N6	91.3(2)
N1–Zn–N6	100.5(2)	N4–Zn–N5	77.6(2)
N2–Zn–N3	74.3(2)	N4–Zn–N6	143.5(2)
N2–Zn–N4	107.2(2)	N5–Zn–N6	88.0(2)
N2–Zn–N5	144.8(2)		

Table 2. Selected Bond Angles (deg) and Distances (Å) for the Metal Coordination Environments in $[\text{Zn}_2(\text{L2H})(\mu\text{-OH})\text{Br}_2](\text{ClO}_4)\text{Br}$ (3)

Zn1–N1	2.032(7)	Zn2–O1	2.104(5)
Zn1–N2	2.218(6)	Zn2–N3	2.143(7)
Zn1–N7	2.478(7)	Zn2–N5	2.142(7)
Br1–Zn1	2.3823(18)	Zn2–N4	2.155(7)
Zn1–O1	1.928(5)	Zn2–Br2	2.3991(17)
N1–Zn1–N2	77.1(3)	N3–Zn2–N4	81.8(3)
N1–Zn1–N7	75.2(3)	N3–Zn2–N5	128.6(3)
N1–Zn1–Br1	106.58(19)	N3–Zn2–Br2	120.26(19)
N1–Zn1–O1	133.9(3)	N3–Zn2–O1	89.6(2)
N2–Zn1–N7	150.2(2)	N4–Zn2–N5	81.4(3)
N2–Zn1–Br1	104.25(17)	N4–Zn2–O1	161.3(3)
N2–Zn1–O1	99.3(2)	N4–Zn2–Br2	97.2(2)
N7–Zn1–O1	92.0(2)	N5–Zn2–Br2	109.9(2)
N7–Zn1–Br1	94.07(19)	N5–Zn2–O1	91.2(2)
O1–Zn1–Br1	118.60(17)	O1–Zn2–Br2	101.53(16)

The crystal structure of complex 3 consists of $[\text{Zn}_2(\text{L2H})(\mu\text{-OH})\text{Br}_2]^{2+}$ cations (Figure 2 and Table 2) and ClO_4^- and Br^- anions. In the binuclear complex the two metal ions, 3.480(2) Å apart, are bridged by an exogenous oxygen atom. In principle, two different formulations can be proposed for this complex: $[\text{Zn}_2(\text{L2H})(\mu\text{-OH})\text{Br}_2]^{2+}$, where an OH^- bridges the two metals while the uncoordinated nitrogen N6 is protonated, or $[\text{Zn}_2\text{L2}(\mu\text{-H}_2\text{O})\text{Br}_2]^{2+}$, with a water molecule bridging the two Zn(II) ions. Actually, the ΔF map did not allow us to locate the protons bound to N6 and O1. On the other hand, the short Zn–O distances (Zn1–O1 1.928(5) Å, Zn2–O1 2.104(5) Å) lead us to propose the former formulation. In fact, several examples of hydroxide anion bridging two Zn(II) metals have been reported, and the Zn–O distances range between 1.9 and 2.1 Å.⁴⁴ Water-bridged dimetal cores are less common, and larger Zn–O distances, ca. 2.3 Å, are found when a water molecule bridges the two metal centers.⁴⁵ At the same time, the Zn–O–Zn angle in water bridged dizinc complexes are lower than 110°,⁴⁵ while by far larger Zn–O–Zn angles are found in

(43) (a) Bencini, A.; Bianchi, A.; Giorgi, G.; Fusi, V.; Masotti, A.; Paoletti, P. *J. Org. Chem.* **2000**, *65*, 7686–7689. (b) Bazzicalupi, C.; Bellusci, A.; Bencini, A.; Berni, E.; Bianchi, A.; Ciattini, S.; Giorgi, G.; Valtancoli, B. *J. Chem. Soc., Dalton Trans.* **2002**, 2151–2157.

(44) A large number of structurally characterized $\mu\text{-OH}$ dizinc complexes have been reported in the literature. Some exemplifying papers are as follows: (a) Bell, M.; Edwards, A. J.; Hoskins, B. F.; Kachab, E. H.; Robson, R. *J. Am. Chem. Soc.* **1989**, *111*, 3603–3610. (b) Grannas, M. J.; Hoskins, B. F.; Robson, R. *Chem. Commun.* **1990**, 1644–1646. (c) Grannas, M. J.; Hoskins, B. F.; Robson, R. *Inorg. Chem.* **1994**, *33*, 1071–1079. (d) Tan, L. H.; Taylor, M. R.; Wainwright, K. P.; Duckworth, P. A. *J. Chem. Soc., Dalton Trans.* **1993**, 2921–2928. (e) Hermann, J.; Erxleben, A. *Inorg. Chim. Acta* **2000**, *304*, 125–129. (f) Bazzicalupi, C.; Bencini, A.; Bianchi, A.; Fusi, V.; Paoletti, P.; Valtancoli, B. *Chem. Commun.* **1994**, 881–882. (g) Bazzicalupi, C.; Bencini, A.; Bianchi, A.; Fusi, V.; Mazzanti, L.; Paoletti, P.; Valtancoli, B. *Inorg. Chem.* **1995**, *34*, 3003–3013. (h) Bazzicalupi, C.; Bencini, A.; Bianchi, A.; Fusi, V.; Paoletti, P.; Piccardi, G.; Valtancoli, B. *Inorg. Chem.* **1995**, *34*, 5622–5630. (i) Asato, E.; Furutachi, H.; Kawahashi, T.; Mikuriya, M. *J. Chem. Soc., Dalton Trans.* **1995**, 3897–3904.

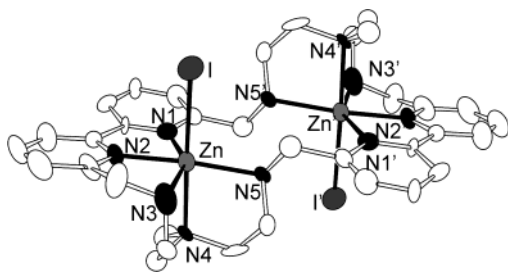


Figure 3. ORTEP drawing of the $[Zn_2L_3I_2]^{2+}$ cation (**6**).

Table 3. Selected Bond Angles (deg) and Distances (Å) for the Metal Coordination Environments in $[Zn_2L_3I_2](ClO_4)_2 \cdot 2H_2O$ (**6**)

Zn–N1	2.35(2)	Zn–N4	2.21(2)
Zn–N2	2.05(2)	Zn–N5	2.22(2)
Zn–N3	2.24(2)	Zn–I	2.818(3)
N1–Zn–N2	73.7(7)	N3–Zn–N5	98.9(7)
N1–Zn–N3	150.8(7)	N4–Zn–N5	81.6(6)
N1–Zn–N4	95.6(6)	N1–Zn–I	87.0(4)
N1–Zn–N5	109.1(6)	N2–Zn–I	87.3(5)
N2–Zn–N3	77.9(7)	N3–Zn–I	98.4(6)
N2–Zn–N4	94.2(7)	N4–Zn–I	177.3(5)
N2–Zn–N5	175.1(7)	N5–Zn–I	96.8(4)
N3–Zn–N4	79.8(7)		

hydroxo-bridged complexes.⁴⁴ Interestingly, the short $N6 \cdots O1$ distance (2.71(1) Å) is indicative of a charge–charge and hydrogen bonding interaction between the ammonium group and the hydroxide anion.

In **3** the two Zn(II) ions display different coordination spheres. Zn1 is coordinated to the heteroaromatic nitrogens (N1 and N2), to the hydroxide O1 and Br1 anions and, at a longer distance, to the benzylic amine N7. The resulting geometry can be best described as a distorted square pyramid. The basal plane is defined by N1, N2, N7, and O1 (max deviation 0.222(7) Å for N1). Zn1 lies 0.616(1) Å above the equatorial plane, shifted toward the apical position occupied by Br1.

The coordination sphere of Zn2, instead, is a distorted trigonal bipyramid where the secondary nitrogens N3 and N5 and the Br2 bromide define the equatorial position, while O1 and N4 occupy the axial positions ($O1–Zn2–N4$ 161.3(3)°).

In **6**, the binuclear cation $[Zn_2L_3I_2]^{2+}$ (Figure 3 and Table 3) lies across an inversion center. Each metal is coordinated to the dipyridine nitrogens, a single triamine chain (N3, N4, and N5) and an exogenous I^- anion, with a distorted octahedral geometry. The heteroaromatic N1 and N2 nitrogens and the benzylic N3 and N5 amines define the equatorial plane (max deviation 0.05(2) Å for N3), while the methylated nitrogen N4 and the iodide anion occupy the apical positions. The two metals, 5.259(2) Å apart, are 0.107(3) Å displaced out of the equatorial plane in the direction of the I^- anion.

The comparison of the crystal structures of the L2 and L3 dinuclear complexes clearly shows that the different number of nitrogen donors and the different cavity size of the two macrocycles strongly affect the coordination environment of

Table 4. Stability Constants (Log K) of the Zn(II) Complexes with L1–L3 (0.1 M NMe_4NO_3 Aqueous Solution) at 308.1 K

reaction	Log K		
	L1	L2	L3
$M^{2+} + L = ML^{2+}$	17.5(1)	12.11(6)	12.69(4)
$ML^{2+} + H^+ = MHL^{3+}$		7.10(6)	9.7(1)
$MHL^{3+} + H^+ = MH_2L^{4+}$		5.22(5)	5.3(1)
$ML^{2+} + OH^- = ML(OH)^+$	3.1(1)	3.05(6)	
		pK_a	
$ML^{2+} + H_2O = ML(OH)^+ + H^+$	10.73	10.78	
$ML^{2+} + M^{2+} = M_2L^{4+}$		4.61(5)	8.79(3)
$M_2L^{4+} + OH^- = M_2L(OH)^{3+}$		6.23(5)	5.05(3)
$M_2L(OH)^{3+} + OH^- = M_2L(OH)_2^{2+}$		5.04(7)	3.63(5)
		pK_a	
$M_2L^{4+} + H_2O = M_2L(OH)^{3+} + H^+$		7.60	8.88
$M_2L(OH)^{3+} + H_2O = M_2L(OH)_2^{2+} + H^+$		8.84	10.1

the metals. While in **3** each metal ion is coordinated to only three ligand donors and completes its coordination sphere binding exogenous species to achieve an overall 5-coordination, in **6** the metal coordination environment is almost saturated by the ligand donors, each metal interacting with five nitrogens. Hexacoordination, however, is achieved through binding of an exogenous iodide anion. At the same time, the larger L3 cavity allows the two metals to lie at a by far larger distance than in the L2 complex (5.259(4) Å in **6** vs 3.480(2) Å in **3**).

Zn(II) Coordination in Aqueous Solution. Table 4 collects the stability constants for the complexes of L1, L2, and L3 with Zn(II), potentiometrically determined in 0.1 mol dm^{-3} NMe_4NO_3 aqueous solution at 308.1 K. Ligand L1 can form only mononuclear complexes in aqueous solution, while L2 and L3 can also form dinuclear complexes, due to the larger dimension of the macrocyclic cavity and to the higher number of nitrogen donors available for metal coordination. The stability of the Zn(II) complex with L1 is remarkably high, among the highest found for Zn(II) complexes with polyamine ligands,^{46,47} suggesting that all of the ligand donors are involved in metal coordination, as actually shown by the crystal structure of the $[ZnL1(NCS)]^+$ cation. In $[ZnL1(NCS)]^+$ the coordination sphere of the metal is completed by a NCS^- anion. Most likely, in aqueous solution the sixth coordinative position is occupied by a water molecule, which can deprotonate at alkaline pH values to give a $[ZnL1(OH)]^+$ species.

As often found in polyamine ligands with a large number (> 6) of amine donors,⁴⁷ the mononuclear $[ZnL2]^{2+}$ and $[ZnL3]^{2+}$ complexes display a marked tendency to add a second metal to give stable dinuclear Zn(II) complexes, which are largely prevalent in aqueous solutions containing Zn(II) and L2 or L3 in 2:1 molar ratio (see Supporting Information) from slightly acidic to alkaline pHs. In particular, the formation of the $[Zn_2L]^{4+}$ species ($L = L2$ or $L3$) occurs at acidic pHs and is followed at neutral or slightly alkaline pH values by the formation of a monohydroxo

(45) Only few examples of μ - H_2O dizinc complexes have been reported: (a) Wolodkiewicz, W.; Glowiak, T. *Pol. J. Chem.* **2001**, *75*, 299–306. (b) Johnson, J. A.; Olmstead, M. M.; Stolzenberg, A. M.; Balch, A. L. *Inorg. Chem.* **2001**, *40*, 5585–5595. (c) Barrios, A. M.; Lippard, S. J. *Inorg. Chem.* **2001**, *40*, 1060–1064.

(46) Bencini, A.; Bianchi, A.; Garcia-España, E.; Mangani, S.; Micheloni, M.; Orioli, P.; Paoletti, P. *Inorg. Chem.* **1988**, *27*, 1104–1107.

(47) Smith, R. M.; Martell, A. E. *NIST Stability Constants Database*, version 4.0; National Institute of Standards and Technology: Washington, DC, 1997.

species $[\text{Zn}_2\text{L}(\text{OH})]^{3+}$. Finally, the formation of a dihydroxo complex, $[\text{Zn}_2\text{L}(\text{OH})_2]^{2+}$, takes place in the alkaline pH region.

At a first glance, these common characteristics for the complexes with L2 and L3 would suggest an almost equal coordination behavior of L2 and L3 toward Zn(II). A more accurate inspection of the formation constants in Table 4, however, reveals some relevant differences in the binding properties of the two ligands. Actually, the mononuclear $[\text{ZnL}_3]^{2+}$ complex displays a much higher tendency to add a second metal to give the $[\text{Zn}_2\text{L}_3]^{4+}$ complex with respect to $[\text{ZnL}_2]^{2+}$ ($\log K = 8.79$ and 4.61 for the equilibrium $[\text{ZnL}]^{2+} + \text{Zn}^{2+} = [\text{Zn}_2\text{L}]^{4+}$, with $L = \text{L}_3$ and L_2 , respectively), in accord with a larger number of N-donors available for the coordination to two Zn(II) cations in L3. Interestingly, the stability of the dinuclear L3 complex is similar to that found for the corresponding complex with the decaazamacrocycle 1,4,7,10,13,16,19,22,25,28-decaazacyclotriacantane (L4), where both the Zn(II) ions are 5-coordinated ($\log K = 21.48$ and 22.5 for the equilibrium $2\text{Zn}^{2+} + L = [\text{Zn}_2\text{L}]^{4+}$ with $L = \text{L}_3$ and L_4 , respectively).⁴⁶ This observation suggests that in the $[\text{Zn}_2\text{L}_3]^{4+}$ complex both metals are coordinated to five nitrogen donors of the macrocycle, as actually observed in the crystal structure of the $[\text{Zn}_2\text{L}_3\text{I}_2]^{2+}$ cation.

In both L2 and L3 dinuclear complexes deprotonation of Zn(II)-coordinated water molecules gives a mono- and a dihydroxo-species. The data in Table 4, however, show that the dinuclear Zn(II) complex with L2 displays a higher tendency to give hydroxo-species than the corresponding L3 complex. In particular, the pK_a value for deprotonation of the first water molecule in $[\text{Zn}_2\text{L}_2]^{4+}$ to give $[\text{Zn}_2\text{L}_2(\text{OH})]^{3+}$ is rather low when compared to the corresponding L3 complex ($pK_a = 7.60$ and 8.88 for $[\text{Zn}_2\text{L}_2]^{4+}$ and $[\text{Zn}_2\text{L}_3]^{4+}$, respectively). Similar low values are generally attributed, in dinuclear Zn(II) complexes, to a bridging coordination of the hydroxide anion between two metal centers. Most likely, in $[\text{Zn}_2\text{L}_2]^{4+}$ the two metals are kept at close distance by the relatively small 21-membered cyclic framework, thus favoring the assembly of a $\text{Zn}_2(\mu\text{-OH})$ unit enclosed in the macrocyclic cavity. This hypothesis is corroborated by the crystal structure of the $[\text{Zn}_2(\text{L}_2\text{H})(\mu\text{-OH})\text{Br}_2]^{2+}$ cation, which shows the two metals only 3.5 \AA apart. The coordination environment of the two metals is not saturated by the ligand donors (each Zn(II) binds to three nitrogens) and is completed through coordination of a bridging hydroxide and of an exogenous bromide anion.

The pK_a value ($8.84 \log$ units) for the formation of $[\text{Zn}_2\text{L}_2(\text{OH})_2]^{2+}$ is too high to be ascribed to a bridging hydroxide anion. Indeed, the bridging hydroxide anion in $[\text{Zn}_2\text{L}_2(\text{OH})]^{3+}$ reduces the positive charge on the metal ions. This would determine the higher pK_a value found for deprotonation of a Zn(II)-bound water molecule to give the $[\text{Zn}_2\text{L}_2(\text{OH})_2]^{2+}$ complex. Similarly, the pK_a values for successive deprotonation of two Zn(II)-bound water molecules in the $[\text{Zn}_2\text{L}_3]^{4+}$ complex to give $[\text{Zn}_2\text{L}_3(\text{OH})]^{3+}$ ($pK_a = 8.88$) and $[\text{Zn}_2\text{L}_3(\text{OH})_2]^{2+}$ ($pK_a = 10.1$) can be related to the formation of single-metal bound hydroxide function. On the other hand,

the larger cavity of ligand L3 would allow the two metals to achieve a larger distance from each other with respect to dinuclear complex with L2. Interestingly, the crystal structure of $[\text{Zn}_2\text{L}_3\text{I}_2]^{2+}$ shows that the intermetallic distance, 5.3 \AA , is too large to allow a bridging coordination mode of hydroxide. At the same time, the coordination sphere of the two Zn(II) ions is rather saturated by the ligand donors, each metal being coordinated to five nitrogens of the macrocycle. The Zn(II) ions, however, achieve an overall hexacoordination by binding to an iodide anion. We can reasonably suppose that, in aqueous solution in absence of added iodide, the I^- ions are replaced by water molecules which can deprotonate in alkaline solutions to give Zn-OH functions.

The dinuclear Zn(II) complexes with L2 and L3 meet the necessary requisites to be used as functional model systems for hydrolytic enzymes. L2 and L3 are capable of holding two metal centers in proximity one to another; the two metals, therefore, may act as a cooperative binding site for substrates. At the same time, facile deprotonation of Zn(II)-bound water molecules occurs at neutral or slightly alkaline pHs to give Zn-OH groups, potential nucleophiles in hydrolytic processes. The dizinc complex with L2 seems, in principle, to be the most promising hydrolytic system; in this complex, in fact, the two metals centers are poorly saturated by the ligand donors, and, therefore, they would give the strongest interaction and activation of the substrates. With this in mind, we decided to investigate the binding properties and the hydrolytic ability of our zinc complexes toward the phosphate ester bond, using bis(*p*-nitrophenyl) phosphate (BNPP) as substrate.

Synthesis and Characterization of the BNPP Complexes. Dinuclear zinc complexes with L2 and L3, $[\text{Zn}_2\text{L}_2](\text{ClO}_4)_4 \cdot 4\text{H}_2\text{O}$ (**2**), and $[\text{Zn}_2\text{L}_3](\text{ClO}_4)_4 \cdot 2\text{H}_2\text{O}$ (**5**) can be isolated as solid compounds from methanol solutions containing the ligands and $\text{Zn}(\text{ClO}_4)_2$ in 1:2 molar ratio. The formation of the ternary complexes between **2** and BNPP was followed by means of ^{31}P NMR spectra recorded on MeOD solutions containing **2** ($1 \cdot 10^{-2} \text{ M}$) and BNPP in different molar ratio. Solutions containing **2** and increasing amounts of BNPP, up to a 1:1 molar ratio, show a single signal 2.9 ppm upfield shifted with respect to that of the “free” ester (Figure 4a). By adding further BNPP, the signal displays a slight downfield shift; a linear correlation between the chemical shift and the $[\text{BNPP}]/[\mathbf{2}]$ ratio is found up to a 2:1 molar ratio (in this condition the signal is 2.68 ppm shifted with respect to free BNPP). A marked downfield shift, instead, is observed for BNPP:**2** molar ratios greater than 2. These data account for the successive formation of stable 1:1 and 1:2 complexes between **2** and BNPP in methanol. The downfield shift observed for $[\text{BNPP}]/[\mathbf{2}] > 2$ is due to the presence in solution of “free” BNPP, fast exchanging, on the NMR time scale, with coordinated BNPP.

From these solutions a solid compound of stoichiometry $[\text{Zn}_2\text{L}_2(\text{BNPP})_2](\text{ClO}_4)_2$ (**4**) was isolated. The rather large shift for the signal of the phosphate ester bound the L2 dinuclear complex would suggest interaction of BNPP with both the Zn(II) ions, through a bridging coordination of the phosphate anion. The ^{31}P NMR spectrum of compound **4** in

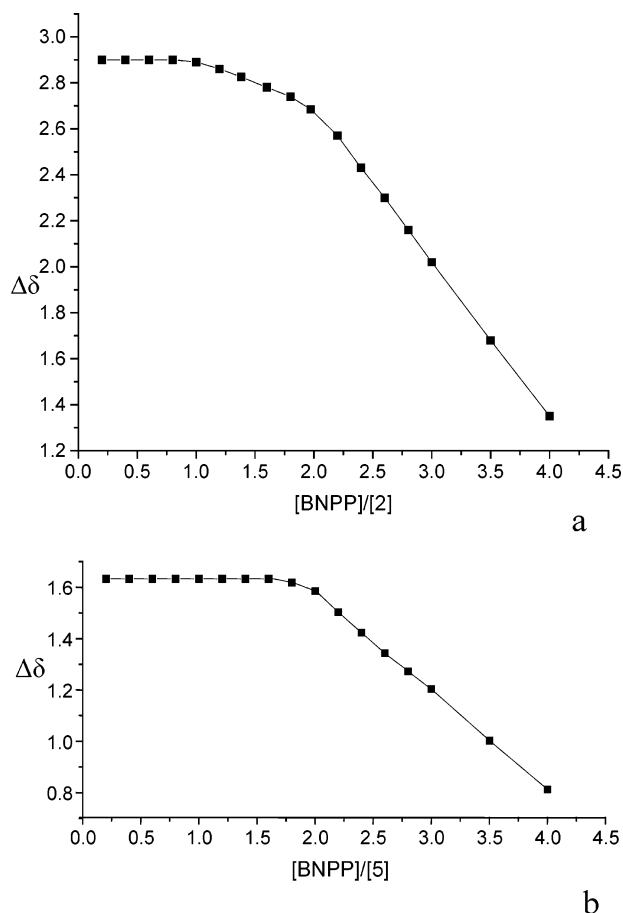


Figure 4. Plot of the ^{31}P NMR chemical shifts of BNPP ($\Delta\delta = \delta_{\text{BNPP}} - \delta_{\text{OBS}}$, where δ_{BNPP} = chemical shift of the unbound BNPP ester and δ_{OBS} = observed chemical shift in the presence of the dinuclear **2** or **5** complexes) as a function of the [BNPP]/[**2**] (a) and of the [BNPP]/[**5**] (b) molar ratios (MeOD solution, 298 K, [**2**] = [**5**] = 1×10^{-2} M).

aqueous solution at neutral pH displays a single signal only 0.41 ppm upfield shifted with respect to unbound BNPP, accounting for a partial decomposition of the complex in this more solvating medium.

In the case of L3, addition of BNPP to a methanol solution of **5** leads to an upfield shift of the BNPP ^{31}P signal, which remains 1.63 ppm shifted up to ca. a **5**:BNPP 1:2 molar ratio (Figure 4b). As in **2**, further addition of BNPP leads to a remarkable downfield shift of the BNPP signal. This behavior suggests the simultaneous addition of two BNPP anions to two almost independent binding sites of **5**, to give a stable $[\text{Zn}_2\text{L3}(\text{BNPP})_2]^{2+}$ complex. In this case, however, the observed upfield shift is lower than that found for the corresponding L2 complex (1.63 and 2.69 ppm in **5** and **2**, respectively), suggesting that in $[\text{Zn}_2\text{L3}(\text{BNPP})_2]^{2+}$ each BNPP anion is bound to a single Zn(II) cation. As in the case of the L2 complex, a minor shift (0.24 ppm) is observed in D_2O solution (pH 7) containing **5** and BNPP in a 1:2 molar ratio, probably due to a much lower percentage of coordinated BNPP in water. However, the solid compound $[\text{Zn}_2\text{L3}(\text{BNPP})_2](\text{BNPP})_2 \cdot 4\text{H}_2\text{O}$ (**7**) was isolated from an aqueous solution containing **5** and an excess of BNPP.

The low temperature crystal structure of **7** consists of $[\text{Zn}_2\text{L3}(\text{BNPP})_2]^{2+}$ cations, unbound BNPP anions, and water

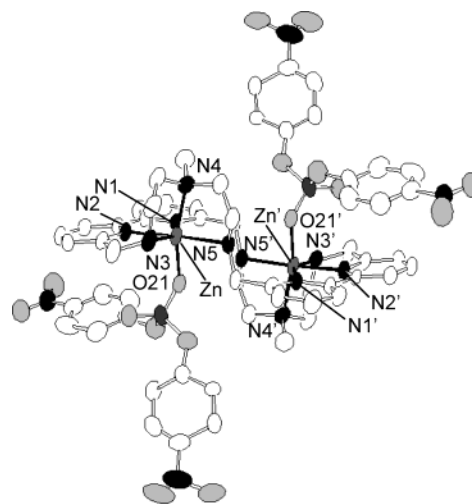


Figure 5. ORTEP drawing of the $[\text{Zn}_2\text{L3}(\text{BNPP})_2]^{2+}$ cation (**7**).

Table 5. Selected Bond Angles (deg) and Distances (\AA) for the Metal Coordination Environment in $[\text{Zn}_2\text{L3}(\text{BNPP})_2](\text{BNPP})_2 \cdot 4\text{H}_2\text{O}$ (**7**)

Zn–N1	2.367(5)	Zn–N4	2.191(6)
Zn–N2	2.086(5)	Zn–N5	2.197(5)
Zn–N3	2.246(5)	Zn–O21	2.085(4)
N1–Zn–N2	73.81(18)	N2–Zn–O21	91.53(19)
N1–Zn–N3	150.83(19)	N3–Zn–N4	81.6(2)
N1–Zn–N4	96.02(18)	N3–Zn–N5	96.75(19)
N1–Zn–N5	111.66(17)	N3–Zn–O21	107.9(2)
N1–Zn–O21	80.70(17)	N4–Zn–N5	80.99(19)
N2–Zn–N3	78.1(2)	N4–Zn–O21	165.93(18)
N2–Zn–N4	100.7(2)	N5–Zn–O21	87.49(17)
N2–Zn–N5	174.17(19)		

molecules. The $[\text{Zn}_2\text{L3}(\text{BNPP})_2]^{2+}$ cation displays two conformations, which differ only for a slightly different orientation of two nitrophenyl groups (see Experimental Section). Figure 5 shows an ORTEP drawing of one of the $[\text{Zn}_2\text{L3}(\text{BNPP})_2]^{2+}$ cations, while Table 5 lists bond angles and distances for the coordination geometry.

The binuclear cation lies across an inversion center. The coordination geometry of each Zn(II) ion is a distorted octahedron, very similar to that found in the $[\text{Zn}_2\text{L3I}_2]^{2+}$ complex (**6**). As in **6**, each metal is coordinated to the dipyrrolic nitrogens and to the three amine groups of a single aliphatic side chain. The heteroaromatic nitrogens (N1 and N2) and the benzylic ones (N3 and N5) define the equatorial plane (max deviation 0.121(7) \AA for N3), while the apical positions are occupied by the methylated nitrogen N4 and the O21 oxygen of one BNPP anion, which behaves as a monodentate ligand and actually replaces the iodide anion in the coordination sphere of Zn(II). The two metals, 5.071(2) \AA apart, lie in the basal planes, slightly shifted (0.039(1) \AA) toward the BNPP oxygens.

Figure 5 shows the presence of a face-to-face π -stacking interaction between a nitrophenyl group of BNPP and an aromatic ring of the dipyrrolic moiety (N2) with an interplanar distance of 3.840(9) \AA .

Despite the many studies on BNPP activation and hydrolysis by Zn(II) complexes,^{25–41} only rare crystal structures of ternary BNPP adducts with Zn(II) have been reported,⁴⁸ regarding mononuclear^{48a–c} or polymeric Zn(II) complexes.^{48d}

Actually, **7** represents the first structurally characterized dinuclear Zn(II) complex with BNPP.

Bis(*p*-nitrophenyl) Phosphate Hydrolysis. The Zn(II) complexes with L1-L3 induce BNPP cleavage, and the hydrolysis products were identified by means of ^1H and ^{31}P NMR measurements. The ^1H NMR spectrum recorded after mixing BNPP and the Zn(II) complexes at pH 10 shows the appearance of the signals of *p*-nitrophenate, NP (two doublets at 6.72 and 8.28 ppm), and of mono(*p*-nitrophenyl) phosphate, MNPP (two doublets at 7.29 and 8.20 ppm). Integration of the signals accounts for a 1:1 molar ratio between the NP and MNPP formed in the hydrolytic process. At the same time, the signal of MNPP (a singlet at $-0.30 \div -0.76$ ppm, depending on the metal complex used) appears in the ^{31}P spectra. The time evolution of the ^{31}P spectra shows a progressive increase of intensity of this signal and a simultaneous decrease of the BNPP signal. No other signal, including that of inorganic phosphate at 3.79 ppm, was observed in ^{31}P NMR spectra, even for prolonged reaction times, indicating the MNPP is not further hydrolyzed by the Zn(II) complexes. Binding and successive hydrolysis of MNPP was recently achieved by Kimura with a dinuclear Zn(II) complex with a propanol-bridged octaazacryptand.^{29,41d} In this case, however, the nucleophilic attack on the substrate was given by an amine group weakly bound to the metal.

The chemical shift of the MNPP signal is 1.02, 1.18, and 1.48 ppm upfield shifted in the presence, respectively, of the $[\text{ZnL1}]^{2+}$, $[\text{Zn}_2\text{L2}]^{4+}$, and $[\text{Zn}_2\text{L3}]^{4+}$ complexes with respect to the signal of MNPP alone at 0.72 ppm, indicating that the MNPP formed in the hydrolytic process is coordinated by the Zn(II) metals. As reported above, the lower upfield shifts, 0.4 ppm or less, are observed for the BNPP signal in the presence of the L1-L3 complexes in aqueous solutions; this comparison suggests a stronger interaction of the MNPP dianion with Zn(II) than BNPP, as expected considering the higher negative charge of MNPP.

The rate constants for BNPP hydrolysis to give MNPP and NP in the presence of the mono- and/or dinuclear complexes with L1-L3 were spectrophotometrically determined at different pH values by an initial slope method, monitoring the time evolution of the NP band at 403 nm. Plots of the absorbance as a function of time show a linear increase of absorbance at 403 nm up to 15–30% formation of *p*-nitrophenate. Then the hydrolysis rate decreased to give finally a total quenching of the cleavage process, due to the inhibition effect of the formed MNPP, more strongly bound to the Zn(II) complexes than BNPP. For instance, at pH 10 with a $[\text{BNPP}]:[\text{Zn complex}]$ 1:1 molar ratio, the percentages of hydrolyzed BNPP at the end of the hydrolytic process were 54%, 49%, and 64% for the L1, L2, and L3 complexes, respectively. Inhibition of the hydrolytic process was also observed with different $[\text{BNPP}]:[\text{Zn complex}]$ molar ratios. These data suggest that MNPP binding inhibits the catalytic

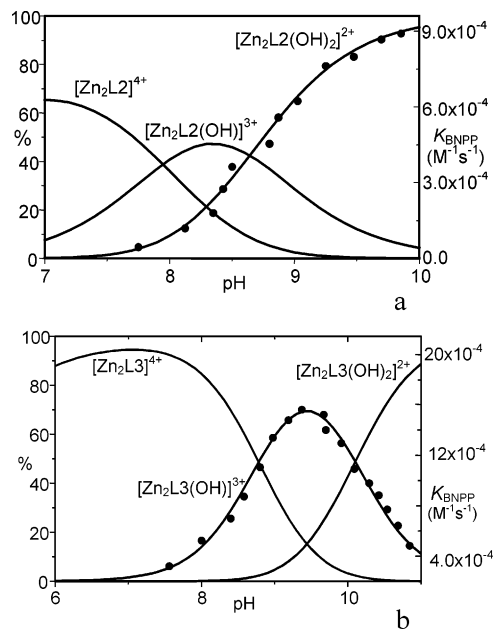


Figure 6. (a) Plot of the distribution curves of the L2 dinuclear complexes (solid line, left Y axis) and k_{BNPP} values for BNPP hydrolysis (●, right Y axis) as a function of pH ($0.1 \text{ mol dm}^{-3} \text{ NMe}_4\text{NO}_3$, 308.1 K). (b) Plot of the distribution curves of the L3 dinuclear complexes (solid line, left Y axis) and k_{BNPP} values for BNPP hydrolysis (●, right Y axis) as a function of pH ($0.1 \text{ mol dm}^{-3} \text{ NMe}_4\text{NO}_3$, 308.1 K).

properties of the complexes. Precipitation of BNPP complexes generally occurs at $[\text{BNPP}]:[\text{Zn complex}]$ molar ratios greater than 10, preventing a Michaelis–Menten analysis of the process. However, the initial linear increase of the absorbance allows one to determine rate constant values (k_{BNPP}) for BNPP cleavage promoted by the L1-L3 Zn(II) complexes. Figure 6 reports the plots of the rate constant values (k_{BNPP}) for the dinuclear Zn(II) complexes with L2 and L3 as a function of pH, superimposed to the corresponding distribution diagrams calculated on the basis of the potentiometric data. For all the systems investigated, only hydroxo-complexes promote BNPP cleavage following second-order kinetics, while the $[\text{ZnL}]^{2+}$ or $[\text{Zn}_2\text{L}]^{4+}$ species are not active, in accord with a mechanism involving a nucleophilic attack of a Zn–OH function. Actually, the mononuclear complex with L3, which does not give any hydroxylated species (Table 4), is totally unable to promote BNPP cleavage. Plots of the k_{BNPP} values as a function of the concentration of the hydroxo-complexes allow for determining k'_{BNPP} values for 100% formation of the active species (see Experimental Section). The active complexes in the hydrolytic process and the corresponding second-order rate constants, k'_{BNPP} , are reported in Table 6. The k'_{BNPP} values for the mononuclear Zn(II) complexes with the tri- and tetraazamacrocycles $[12]\text{aneN}_3$ and $[12]\text{aneN}_4$ ⁴⁹ and for the dinuclear Zn(II) complexes with macrocycles $[30]\text{aneN}_6\text{O}_4$,^{37a} $[33]\text{aneN}_7\text{O}_4$,^{37c} and $[36]\text{aneN}_8\text{O}_4$,^{37c} which contain two separated triamine or tetraamine binding units, are also reported for comparison.

BNPP hydrolysis promoted by mono- and dinuclear Zn(II) complexes is generally explained in terms of an “as-

(48) (a) Weiss, K.; Rombach, M.; M. Ruf, Vahrenkamp, H. *Eur. J. Inorg. Chem.* **1998**, 263–270. (b) Yamami, M.; Furutachi, H.; Yokoyama, T.; Okawa, H. *Chem. Lett.* **1998**, 211–212. (c) Ibrahim, M. M.; Shimomura, N.; Ichikawa, K.; Shiro, M. *Inorg. Chim. Acta* **2001**, 125–136. (d) Angeloff, A.; Daran, J. C.; Bernadou, J.; Meunier, B. *J. Organometallic Chem.* **2001**, 624, 58–62.

(49) Koike, T.; Kimura, E.; *J. Am. Chem. Soc.* **1991**, 113, 8935–8941.

Table 6. Second-Order Rate Constants k'_{BNPP} ($\text{M}^{-1} \text{s}^{-1}$) for Hydrolysis of Bis(*p*-nitrophenyl) Phosphate and $\text{p}K_{\text{a}}$ Values for the Corresponding Hydroxo-Complexes at 308.1 K

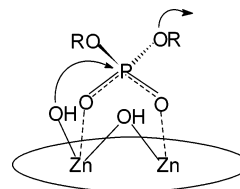
nucleophile	$k'_{\text{BNPP}} \times 10^4$ ($\text{M}^{-1}\text{s}^{-1}$)	$\text{p}K_{\text{a}}$	nucleophile	$k'_{\text{BNPP}} \times 10^4$ ($\text{M}^{-1}\text{s}^{-1}$)	$\text{p}K_{\text{a}}$
$[\text{ZnL1}(\text{OH})]^+$	1.1 ± 0.06	10.73	$[\text{Zn}[12]\text{aneN}_3(\text{OH})]^+{}^a$	0.85	7.2
$[\text{ZnL2}(\text{OH})]^+$	1.5 ± 0.08	10.78	$[\text{Zn}[12]\text{aneN}_4(\text{OH})]^+{}^a$	0.21	8.1
$[\text{Zn}_2\text{L2}(\text{OH})]^{3+}$	not active	7.60	$[\text{Zn}_2[30]\text{aneN}_6\text{O}_4(\text{OH})_2]^{2+b}$	1.15	9.2
$[\text{Zn}_2\text{L2}(\text{OH})_2]^{2+}$	9.6 ± 0.3	8.84	$[\text{Zn}_2[33]\text{aneN}_7\text{O}_4(\text{OH})_2]^{2+c}$	0.91	9.38
$[\text{Zn}_2\text{L3}(\text{OH})]^{3+}$	19.3 ± 1.0	8.88	$[\text{Zn}_2[36]\text{aneN}_8\text{O}_4(\text{OH})_2]^{2+c}$	0.54	9.88
$[\text{Zn}_2\text{L3}(\text{OH})_2]^{2+}$	not active	10.1			

^a From ref 49, I = 0.15 M NaClO_4 . ^b From ref 37a, I = 0.1 M NaCl . ^c From ref 37c, I = 0.1 M NaCl

sociative” mechanism,^{26–40,50} in which the substrate would approach the Zn(II) complex and the oxygens of BNPP associate with the electrophilic Zn(II) ion. Finally, a zinc-bound hydroxide operates a nucleophilic attack at the phosphorus. The hydrolytic activity of a complex, therefore, is enhanced by a strong interaction of the BNPP ester with the electrophilic metal centers and by a high nucleophilic character of the Zn–OH functions, i.e., by high $\text{p}K_{\text{a}}$ values for the formation of the Zn-bound hydroxide.

Considering the dinuclear Zn(II) complexes with L2, the plot of the second-order rate constants k_{BNPP} for the Zn/L2 (2:1 molar ratio) system as a function of pH points out that only the dihydroxo complex $[\text{Zn}_2\text{L2}(\text{OH})_2]^{2+}$ promotes BNPP hydrolysis in aqueous solution, i.e., $[\text{Zn}_2\text{L2}(\text{OH})_2]^{2+}$ is the kinetically active species (Figure 6a). On the contrary the monohydroxo complex $[\text{Zn}_2\text{L2}(\text{OH})]^{3+}$ is totally inactive.

As already found with other binucleating ligands,³⁷ the lack of hydrolytic ability of the $[\text{Zn}_2\text{L2}(\text{OH})]^{3+}$ species can be attributed to a bridging coordination of the hydroxide anion to two electrophilic metal centers which reduces the nucleophilicity of the generated hydroxide function. The dinuclear L2 complex $[\text{Zn}_2\text{L2}(\text{OH})_2]^{2+}$, instead, exhibits a remarkably higher hydrolytic ability than the mononuclear L2 and L1 complexes $[\text{ZnL2}(\text{OH})]^+$ and $[\text{ZnL1}(\text{OH})]^+$ (Table 6). This behavior cannot be explained in terms of nucleophilic ability of the Zn–OH functions, since the $\text{p}K_{\text{a}}$ values for the formation of the mononuclear complexes $[\text{ZnL2}(\text{OH})]^+$ and $[\text{ZnL1}(\text{OH})]^+$ are by far higher than the $\text{p}K_{\text{a}}$ value for the dinuclear $[\text{Zn}_2\text{L2}(\text{OH})_2]^{2+}$ complex, i.e., the Zn–OH function is more nucleophile in $[\text{ZnL2}(\text{OH})]^+$ and $[\text{ZnL1}(\text{OH})]^+$ than in $[\text{Zn}_2\text{L2}(\text{OH})_2]^{2+}$. The high activity of the $[\text{Zn}_2\text{L2}(\text{OH})_2]^{2+}$ would be explained, instead, by a cooperative role of the two metals in the hydrolytic process, which takes place via a bridging interaction of BNPP, as actually suggested by the ³¹P NMR measurements. Substrate interaction with two electrophilic metal centers, in fact, favors the nucleophilic attack of a Zn–OH function and thus enhances the rate of the hydrolytic process, as found in

**Figure 7.** Proposed mechanism for BNPP hydrolysis promoted by the dinuclear Zn(II) complex with L2.

several dinuclear synthetic Zn(II) complexes.^{26–40} As discussed above, in the dinuclear L2 complexes the two metals are kept at a short distance by the rather small macrocyclic cavity, and, at the same time, the coordination sphere of both metals is poorly saturated by the ligand donors. These structural features would favor a bridging interaction mode of the phosphate ester. A sketch of the proposed hydrolytic mechanism is shown in Figure 7.

The dinuclear Zn(II) complexes with L3 display an inverse behavior in BNPP cleavage with respect to the L2 ones. According to Figure 6b, in fact, only the monohydroxo complex $[\text{Zn}_2\text{L3}(\text{OH})]^{3+}$ promotes BNPP hydrolysis, while $[\text{Zn}_2\text{L3}(\text{OH})_2]^{2+}$ is totally inactive. As shown in Table 6, the $[\text{Zn}_2\text{L3}(\text{OH})]^{3+}$ complex is more active than the mononuclear L1 and L2 complexes and even more than the dinuclear $[\text{Zn}_2\text{L2}(\text{OH})_2]^{2+}$ one, suggesting that in $[\text{Zn}_2\text{L3}(\text{OH})]^{3+}$ the two metals still work cooperatively in BNPP hydrolysis. On the other hand, the crystal structures of the $[\text{Zn}_2\text{L3I}_2]^{2+}$ and $[\text{Zn}_2\text{L3}(\text{BNPP})_2]^{2+}$ anions show that each metal cation is coordinated to five nitrogen donors of the macrocycle and achieves hexacoordination by binding to an iodide or a BNPP anion. Coordination numbers greater than 6 are extremely rare in Zn(II) chemistry; at the same time, the $\text{p}K_{\text{a}}$ values for water deprotonation to give the $[\text{Zn}_2\text{L3}(\text{OH})]^{3+}$ and $[\text{Zn}_2\text{L3}(\text{OH})_2]^{2+}$ species account for the formation of single-metal bound OH^- functions. Therefore, in the monohydroxo complex one Zn(II) ion is characterized by a coordination sphere saturated by five ligand donors and the OH^- anion, while the second metal possesses a free binding site for BNPP coordination. The simultaneous presence within the same complex of both a binding site for BNPP and a nucleophilic Zn–OH function in proximity would account for the hydrolytic ability of the $[\text{Zn}_2\text{L3}(\text{OH})]^{3+}$ complex, as sketched in Figure 8. In the $[\text{Zn}_2\text{L3}(\text{OH})_2]^{2+}$ complex both Zn(II) would have a coordination environment saturated by the ligand donors and the hydroxide anions and no binding sites are available for the interaction with BNPP. In consequence, this species is not active in BNPP hydrolysis.

(50) (a) Yashiro, M.; Ishikubo, A.; Komiyama, M. *J. Chem. Soc., Chem. Commun.* **1995**, 1793–1794. (b) Kondo, S.; Shinbo, K.; Yamaguchi, T.; Yoshida, K.; Yano, Y. *J. Chem. Soc., Perkin Trans. 2* **2001**, 128–135. (c) Kawahara S.; Uchimaru, T. *Eur. J. Inorg. Chem.* **2001**, 2437–2442. (d) Yamada, K.; Takahashi, Y.; Yamamura, H.; Araki, S.; Saito, K.; Kawai, M. *Chem. Commun.* **2000**, 1315–1310. (e) Matsuda, S.; Yashiro, M.; Kuzuka, A.; Ishikubo, A.; Komiyama, M. *Angew. Chem., Int. Ed. Eng.* **1998**, 37, 3284–3286.

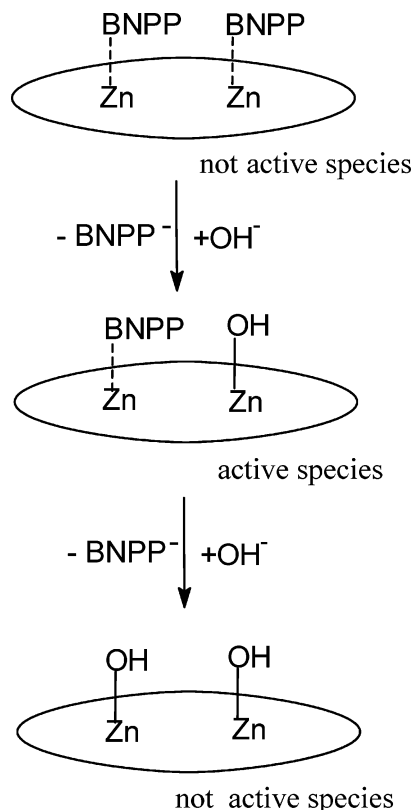


Figure 8. Schematic representation of the L3 complexes involved in BNPP activation and hydrolysis.

In comparison with previously reported dizinc complexes containing hydrolytic Zn–OH functions, the L2 and L3 dinuclear complexes show a high activity in BNPP cleavage. To our knowledge, only the dizinc complex with a bis-macrocyclic composed of two [9]aneN₃ units linked by a quinoxaline linkage displays a higher activity.⁵¹ In this case, however, the hydrolysis occurs only at strongly alkaline pHs, where a highly nucleophilic trihydroxo complex is formed in solution. These observations suggest that the insertion of dipyrindine unit(s) within a macrocyclic structure enhances the hydrolytic ability of the complexes. Actually, the crystal structure of the $[\text{Zn}_2\text{L3}(\text{BNPP})_2]^{2+}$ complex shows that BNPP also interacts with the L3 complex via π -stacking interactions between the nitrophenyl groups and the dipyrindine moieties. This structural feature suggests that the high activity of the present complexes may be related to π -stacking and/or hydrophobic interactions between BNPP and the zinc complexes, which can strengthen the association between the L2 and L3 complexes and the substrate in the transient state of the hydrolytic mechanism, thus enhancing the hydrolysis rate. The presence of two dipyrindine moieties in L3, which increases the hydrophobic characteristics of the ligand with respect to L2, would also explain the higher hydrolytic ability of the L3 dinuclear complex.

Conclusions

The dipyrindine-containing macrocycles L2 and L3 form stable dizinc complexes in aqueous solution, and, in both cases, deprotonation of Zn-bound water molecules generates Zn–OH functions able to hydrolyze the BNPP ester.

With respect to previously reported dinuclear Zn(II) complexes, the present ones present two peculiar characteristics: first, the presence of dipyrindine binding units within the macrocyclic framework leads to a marked increase of the hydrolysis ability of the complexes. This effect may be related to the hydrophobic nature of this heteroaromatic unit, which would increase the interaction between the host complex and the substrate through π -stacking and hydrophobic interactions. Second, the hydrolytic mechanism is modulated by the different molecular topology of the two ligands such as the number of donors and dimension of the macrocyclic cavity. In the dinuclear L2 complex the two metals are kept at close distance by the smaller macrocyclic cavity, and only a few nitrogens are involved in metal coordination. Therefore, several free coordination sites are available for the binding of exogenous species. In the corresponding L3 complex the metals are hosted by two separated binding moieties, and their coordination sphere is rather saturated by the ligand donors, each metal being coordinated to five nitrogens. In the L3 complex, however, each metal can achieve hexacoordination through the binding of an exogenous species. In both complexes the two metals play a cooperative role in phosphate ester cleavage. In BNPP cleavage by the L2 complex both metals participate in substrate binding and activation, through a bridging coordination of the ester. In the case of the L3 complex a less common mechanism is at work; in fact, BNPP interacts with a single metal cation of the $[\text{Zn}_2\text{L3}(\text{OH})]^{3+}$ complex, while the hydroxide anion operates the nucleophilic attack at phosphorus.

Experimental Section

General Procedures. Ligand L1, L2, and L3 were obtained as previously reported.⁴³ UV–vis spectra were recorded on a Shimadzu UV-2101PC spectrophotometer. ³¹P and ¹H NMR spectra were recorded on VARIAN 300 MHz instrument.

Synthesis of the Complexes. $[\text{ZnL1}(\text{NCS})]\text{ClO}_4$ (**1**). A solution of $\text{Zn}(\text{ClO}_4)_2 \cdot 6\text{H}_2\text{O}$ (11.3 mg, 0.030 mmol) in water (5 mL) was slowly added under stirring to an aqueous solution (10 mL) of L1 (8.9 mg, 0.030 mmol). NaSCN (2.4 mg, 0.030 mmol) and NaClO₄ (50 mg) were then added. Colorless crystals of the title compound suitable for X-ray diffraction analysis were obtained by slow evaporation at room temperature of the resulting solution. Yield 7.3 mg (47%). Elemental anal. Found: C, 41.6; H, 4.48; N, 16.13. Calcd for C₁₈H₂₅ZnN₆SClO₄: C, 41.55; H, 4.45; N, 16.15.

$[\text{Zn}_2\text{L2}](\text{ClO}_4)_4 \cdot 4\text{H}_2\text{O}$ (**2**). A solution of $\text{Zn}(\text{ClO}_4)_2 \cdot 6\text{H}_2\text{O}$ (20.2 mg, 0.054 mmol) in MeOH (5 mL) was added to a methanol solution (5 mL) of L2 (10 mg, 0.027 mmol). Butanol (15 mL) was then added, affording the title compound as colorless solid. Yield 20.2 mg (74%). Elemental anal. Found: C, 24.5; H, 4.1; N, 10.22. Calcd for C₂₀H₃₉Zn₂N₇Cl₄O₂₀: C, 24.76; H, 4.05; N, 10.11.

$[\text{Zn}_2(\text{L2H})(\mu\text{-OH})\text{Br}_2](\text{ClO}_4)\text{Br}$ (**3**). An aqueous solution (5 mL) of NaBr (15 mg, 0.14 mmol) was slowly added to an aqueous solution of complex **2** (15 mg, 0.0154 mmol), and the resulting solution was stirred for ca. 2 h. Colorless crystals of the complex suitable for X-ray diffraction analysis were obtained by slow

(51) Arca, M.; Bencini, A.; Berni, E.; Caltagirone, C.; Devillanova, F. A.; Isaia, F.; Garau, A.; Giorgi, G.; Lippolis, V.; Perla, A.; Tei, L.; Valtancoli, B. *Inorg. Chem.* **2003**, *42*, 6929–6939.

evaporation at room temperature. Yield 7.2 mg (54%). Elemental anal. Found: C, 28.1; H, 4.2; N, 11.42. Calcd for $C_{20}H_{33}Br_3Zn_2N_7-ClO_5$: C, 28.01; H, 3.88; N, 11.43.

[Zn₂L2(BNPP)₂](ClO₄)₂ (4). A solution of NaBNPP (11.2 mg, 0.031 mmol) in methanol (5 mL) was added to a methanol solution of complex **2** (15 mg, 0.0154 mmol), and the resulting solution was stirred for ca. 1 h. Addition of butanol (15 mL) afforded a colorless powder. Yield 3.7 mg (18%). Elemental anal. Found: C, 38.5; H, 3.6; N, 11.1; Cl, 5.15; P, 4.50. Calcd for $C_{44}H_{47}Zn_2N_{11}-Cl_2O_{24}P_2$: C, 38.36; H, 3.44; N, 11.18; Cl, 5.3; P, 4.3;

[Zn₂L3](ClO₄)₄·2H₂O (5). This compound was obtained in 83% by using the same procedure used for **2**. Elemental anal. Found: C, 35.4; H, 4.5; N, 12.2. Calcd for $C_{34}H_{50}Zn_2N_{10}Cl_4O_{18}$: C, 35.22; H, 4.35; N, 12.08.

[Zn₂L3I₂](ClO₄)₂·2H₂O (6). This complex was obtained by following the same procedure used for **3**, by addition of NaI instead of NaBr to an aqueous solution of complex **5**. Yield 5.5 mg (33%). Elemental anal. Found: C, 33.8; H, 4.1; N, 11.6. Calcd for $C_{34}H_{50}I_2-Zn_2N_{10}Cl_2O_{10}$: C, 33.63; H, 4.15; N, 11.53.

[Zn₂L3(BNPP)₂](BNPP)₂·4H₂O (7). A solution of $Zn(ClO_4)_2·6H_2O$ (21.2 mg, 0.056 mmol) in water (15 mL) was slowly added to an aqueous solution (15 mL) of L3 (16.6 mg, 0.028 mmol). NaBNPP (101.4 mg, 0.28 mmol) was then added, and the resulting solution was refrigerated at 5 °C. Colorless crystals, suitable for X-ray diffraction analysis, were obtained by slow evaporation at 5 °C. Yield 32.7 mg (55%). Elemental anal. Found: C, 45.8; H, 4.2; N, 11.8; P, 5.6. Calcd for $C_{82}H_{86}Zn_2N_{18}O_{36}P_4$: C, 45.72; H, 4.02; N, 11.70; P, 5.75.

Potentiometric Measurements. Equilibrium constants for complexation reactions with L1, L2, and L3 were determined by means of potentiometric measurements ($pH = -\log [H^+]$), carried out in 0.1 mol dm⁻³ NMe_4NO_3 at 308.1 ± 0.1 K, in the pH range 2.5–11, by using the equipment that has been already described.⁵² The reference electrode was an Ag/AgCl electrode in saturated KCl solution. The glass electrode was calibrated as a hydrogen concentration probe by titrating known amounts of HCl with CO₂-free NaOH solutions and determining the equivalent point by the Gran's method.⁵³ This allows one to determine the standard potential E° and the ionic product of water ($pK_w = 13.40 \pm 0.01$). Ligand concentration was about 1×10^{-3} M, while metal concentration was in the range 2×10^{-3} – 5×10^{-4} M. At least three measurements (about 100 experimental points each one) were performed for each system. The computer program HYPERQUAD⁵⁴ was used to calculate the protonation constants and the stability constants of Zn(II) complexes from emf data. Ligands protonation constants at 308.1 K are supplied within the Supporting Information. The titration curves for each system were treated either as a single set or as separated entities without significant variations in the values of the protonation or metal complexation constants. In the HYPERQUAD program the sum of the weighted square residuals on the observed emf values is minimized. The weights were derived from the estimated errors in emf (0.2 mV) and titrant volume (0.002 cm³). The most probable chemical model was selected by following a strategy based on the statistical inferences applied to the variance of the residuals, σ^2 . This parameter represents a measure of the precision of the fit between the experimental and theoretical titration curves. The sample standard deviation should be 1, in the absence

of systematic errors and when a corrected weighting scheme is used. However, the agreement is considered good for standard deviation values smaller than 3 ($\sigma^2 < 9$).⁵⁵ The σ^2 values for each titration curve and for the overall set of curves of each system are reported within the Supporting Information.

Kinetics of Bis(p-nitrophenyl)phosphate (BNPP) Hydrolysis. The hydrolysis rate of BNPP to give mono(p-nitrophenyl) phosphate (MNPP) and p-nitrophenate (the hydrolysis products were identified by means of ¹H and ³¹P NMR spectra) in the presence of the zinc complexes with L1, L2, and L3 was measured by an initial slope method monitoring the increase in 403 nm absorption of the p-nitrophenate at 308.1 ± 0.1 K using the procedure reported in ref 37. The ionic strength was adjusted to 0.1 with NMe_4NO_3 . The reaction solution was maintained at 308.1 ± 0.1 K. MOPS (pH 6.5–8.5), TAPS (pH 7.8–9.1), CHES (pH 8.6–10.1), and CAPS (pH 9.7–11.1) buffers were used (50 mM). Freshly prepared stock solutions of the complexes (1–10 mM) and of BNPP (1–10 mM) were used in the measurements. In a typical experiment, immediately after BNPP and the zinc complexes with L1–L3 were mixed in aqueous solutions at the appropriate pH (the reference experiment does not contain the Zn(II) complex), the UV absorption spectrum was recorded and followed generally until 5–10% decay of BNPP. A plot of the hydrolysis rate vs BNPP concentration (1–10 mM) at a given pH gave a straight line, and then we determine the slope/[zinc complex] as the second-order rate constants k_{BNPP} (M⁻¹ s⁻¹). Plots of the k_{BNPP} values as a function respectively of the molar concentrations of the active species ([ZnL1(OH)]⁺, [ZnL2(OH)]⁺, [ZnL2(OH)₂]²⁺, or [ZnL3(OH)]³⁺) give straight lines and allow for determining the k'_{BNPP} values for 100% formation of [ZnL1(OH)]⁺, [ZnL2(OH)]⁺, [ZnL2(OH)₂]²⁺, and [ZnL3(OH)]³⁺. Errors in k'_{BNPP} values were about 5%.

Single-Crystal X-ray Diffraction Analyses. Single crystals of [ZnL1(NCS)]ClO₄ (**1**), [Zn₂(L2H)(μ-OH)Br₂](ClO₄)Br (**3**), [Zn₂-L3I₂](ClO₄)₂·2H₂O (**6**), and [Zn₂L3(BNPP)₂](BNPP)₂·4H₂O (**7**) were analyzed by means of X-ray crystallography, and a summary of the crystallographic data is reported in Table 7. The intensities of two reflections were monitored during data collections to check the stability of the crystals: no loss of intensity was observed. The integrated intensities were corrected for Lorentz and polarization effects and empirical absorption corrections were applied by means of the PSI-SCAN method (**1**, **3**, and **6**) and of the SADABS program (**7**).⁵⁶ All the structures were solved by direct methods (SIR97).⁵⁷ Refinements were performed by means of full-matrix least-squares using SHELX-97 program.⁵⁸ In each structure all the non-hydrogen atoms were anisotropically refined, while the hydrogen atoms were introduced in a calculated position and their coordinates were refined according to the linked atoms.

1. Rotational disorder affects the perchlorate anion which was interpreted by means of two tetrahedral models (Cl1–O1A, O2A, O3A, O4A and O1B, O2B, O3B, O4B) with a population parameter of 0.5.

6. Crystals of this compound were of rather low quality. This accounts for the high values of the agreement factors at the end of refinement and of the thermal parameters for some atoms. Several attempts to obtain crystals of better quality did not give good results.

(52) Bianchi, A.; Bologni, L.; Dapporto, P.; Micheloni, M.; Paoletti, P. *Inorg. Chem.* **1984**, *23*, 1201–1207.

(53) (a) Gran, G. *Analyst (London)* **1952**, *77*, 661–663. (b) Rossotti, F. J.; Rossotti, H. J. *Chem. Educ.* **1965**, *42*, 375–378.

(54) Gans, P.; Sabatini, A.; Vacca, A. *J. Chem. Soc., Dalton Trans.* **1985**, 1195–1200.

(55) (a) Hamilton, W. C. *Statistics in Physical Chemistry*; The Ronald Press Company; New York, U.S.A., 1964. (b) Bologni, L.; Sabatini, A.; Vacca, A. *Inorg. Chim. Acta* **1983**, *69*, 71–75.

(56) Bruker Molecular Analysis Research Tool, Vers. 5.625, Bruker AXS, Madison, WI, 1997–2000.

(57) Altomare, A.; Burla, M. C.; Camalli, M.; Cascarano, G. L.; Giacovazzo, C.; Guagliardi, A.; Moliterni, A. G. G.; Polidori, G.; Spagna, R. *J. Appl. Crystallogr.* **1999**, *32*, 115–119.

(58) G. M. Sheldrick, *SHELXL-97*, Göttingen, 1997.

Table 7. Crystal Data and Structure Refinement for [ZnL1(NCS)]ClO₄ (**1**), [Zn₂(L2H)(μ-OH)Br₂](ClO₄)Br (**3**), [Zn₂L3I₂](ClO₄)₂·2H₂O (**6**), and [Zn₂L3(BNPP)₂](BNPP)₂·4H₂O (**7**)

	1	3	6	7
empirical formula	C ₁₈ H ₂₃ ClN ₆ O ₄ SZn	C ₂₀ H ₃₃ Br ₃ ClN ₇ O ₅ Zn ₂	C ₃₄ H ₅₀ Cl ₂ I ₂ N ₁₀ O ₁₀ Zn ₂	C ₈₂ H ₈₆ N ₁₈ O ₃₆ P ₄ Zn ₂
formula weight	520.30	857.45	1214.28	2154.30
temperature (K)	298	298	298	170
wavelength (Å)	0.71069	1.5418	0.71069	1.5418
collecting equipment	Enraf-nonius CAD4	Brucker P4	Brucker P4	Brucker CCD
space group	<i>P</i> 2 ₁ / <i>n</i>	<i>P</i> 1̄	<i>P</i> 1̄	<i>P</i> 1̄
<i>a</i> (Å)	14.601(3)	11.375(4)	8.378(2)	11.394(5)
<i>b</i> (Å)	10.808(3)	7.919(4)	11.532(4)	13.395(5)
<i>c</i> (Å)	15.685(3)	17.335(5)	12.684(4)	16.396(5)
α (deg)		84.12(3)	75.57(2)	66.670(5)
β (deg)	116.63(2)	76.53(2)	75.05(3)	81.070(5)
γ (deg)		98.94(6)	80.89(2)	83.040(5)
volume (Å ³)	2212.6(9)	1484.5(10)	1140.8(6)	2265.0(15)
<i>Z</i>	4	2	1	1
<i>D</i> _{calcd} (Mg/m ³)	1.562	1.918	1.767	1.579
μ (mm ⁻¹)	1.363	7.918	2.584	2.189
R indices [<i>I</i> > 2σ(<i>I</i>)] ^a	R1 = 0.0612 wR2 = 0.1568	R1 = 0.0538 wR2 = 0.1475	R1 = 0.0940 wR2 = 0.2378	R1 = 0.0735 wR2 = 0.2042
R indices (all data) ^a	R1 = 0.1126 wR2 = 0.1844	R1 = 0.0599 wR2 = 0.1560	R1 = 0.1252 wR2 = 0.2582	R1 = 0.0809 wR2 = 0.2114

$$^a \text{R1} = \sum |F_o| - |F_c| / \sum |F_o|; \text{wR2} = [\sum w(F_o^2 - F_c^2)^2 / \sum wF_o^4]^{1/2}.$$

Disorder or thermal motion affects the water molecules. Two different locations were determined for the oxygen atoms (O10 and O10') and refined with a population parameter of 0.5. Residual electron density (largest diff. peak and hole 1.333 and -0.969 eÅ⁻³) was found at the end of refinement.

7. Two conformations, with a population parameter of 0.5, were found for complex **7**. They differ only for slightly different orientations of two nitrophenyl groups, belonging respectively one to the coordinated (C19–C23, O61, O62) and the other one to the not bound BNPP anion (C31–C35, O81, O82). In both cases the aromatic rings are rotated on the axis linking the 1,4 positions of the benzene units.

Acknowledgment. Financial support by the Italian Ministero dell'Università e della Ricerca Scientifica e Tecnologica (COFIN 2002) is gratefully acknowledged.

Supporting Information Available: Ligands protonation constants determined in 0.1 mol dm⁻³ NMe₄NO₃ solutions at 308.1 K, values of the variance of weighted square residuals for the potentiometric curves, distribution diagrams for the systems L2/Zn²⁺ and L3/Zn²⁺ with a ligand to metal 1:2 molar ratio, and crystal packing of [Zn₂L3(BNPP)₂](BNPP)₂·4H₂O (**7**), CCDC-223741, 223742, 223743, and 223744 for compounds **1**, **3**, **6**, and **7**, respectively, contain the crystallographic data. These data can be obtained free of charge at www.ccdc.cam.ac.uk/conts/retrieving.html [or from the Cambridge Crystallographic Data Centre, 12, Union Road, Cambridge CB2 1EZ, UK; fax: (internat.) +44-1223/336-033; E-mail: deposit@ccdc.cam.ac.uk]. This material is available free of charge via the Internet at <http://pubs.acs.org>.

IC049754V